S
E
C
R
U
O
S
E
R

L
A
R
U
T
A
N

Development of Design Guidelines for Structures that Serve as Tsunami Vertical Evacuation Sites

by Harry Yeh,
Ian Robertson,
and Jane Preuss

This report has not been edited or reviewed for conformity with Division of Geology and Earth Resources standards and nomenclature

WASHINGTON STATE DEPARTMENT OF
Natural Resources
Doug Sutherland - Commissioner of Public Lands

Development of Design Guidelines for Structures that Serve as Tsunami Vertical Evacuation Sites

by Harry Yeh,
Ian Robertson,
and Jane Preuss

This report has not been edited or reviewed for conformity with Division of Geology and Earth Resources standards and nomenclature

WASHINGTON STATE DEPARTMENT OF
Natural Resources
Doug Sutherland - Commissioner of Public Lands

Contents

FIGURES

TABLES

FOREWORD

The National Tsunami Hazard Mitigation Program (NTHMP) was created by Congress in October 1996 and is a partnership of the five Pacific Coast states, the National Oceanic and Atmospheric Administration (NOAA), the Federal Emergency Management Agency (FEMA), and the U.S. Geological Survey (USGS). The NTHMP is designed to reduce the impact of tsunamis through warning guidance, hazard assessment, and mitigation (see http://www.pmel.noaa.gov/tsunami-hazard/index.htm). Its strategic implementation plan for tsunami mitigation projects (Dengler, 1998) identified construction guidelines and coastal land use guidance in areas of both strong ground shaking and tsunami hazard as a primary need throughout the region. In November 2002, a workshop was held in Seattle, Washington, with attendees having expertise in structural, marine, and civil engineering, seismology, geology, and emergency management to assess the feasibility of such guidance and to formulate a plan for its development (Walsh and others, 2002).

A two-phase program was recommended. The purpose of Phase I was to extract data from unpublished tsunami surveys to estimate forces from tsunami waves on buildings, to analyze buildings that survived tsunami wave attack, and to test those forces against building code designs. This report is an account of work on Phase I performed under contracts E04-001 and E04-130 to the Washington State Military Department, Emergency Management Division, on behalf of the NTHMP.

Phase II will build on Phase I results to develop design and siting specifications, a manual for field data collections, and an outreach program consisting of the creation of databases and a series of workshops to disseminate and train design professionals in the application of the guidelines. The Phase II contract has been let to the Applied Technology Council of Redwood City, California, under contract to the Federal Emergency Management Agency, and is anticipated to be completed in 2006 or 2007.

TIMOTHY J. WALSH

References Cited

Dengler, L. A., 1998, Strategic implementation plan for tsunami mitigation projects: U.S. National Oceanic and Atmospheric Administration Technical Memorandum ERL PMEL-113, 133 p. [Available at http://www.pmel.noaa.gov/pubs/PDF/deng2030/deng2030.pdf]

Walsh, T. J.; Crawford, George; Eisner, Richard; Preuss, J. V., 2002, Proceedings of a workshop on construction guidance for areas of high seismic and tsunami loading: Washington Emergency Management Division, 25 p.

Development of Design Guidelines
for Structures that Serve as Tsunami Vertical Evacuation Sites
(52-AB-NR-200051)

By

Harry Yeh, Oregon State University
Ian Robertson, University of Hawaii
Jane Preuss, Planwest Partners

This is a report of an exploratory study for the development of standards and guidelines for building safely against combined seismic-tsunami loads. Unlike seismic ground shaking, tsunami effects are limited to its inundation zone, and the closer to the shore the more severe the destruction. The present wet-or-dry presentation of the tsunami hazard maps must be improved to identify the multiple influence zones: e.g. high, medium, and low tsunami force zones in terms of both human survival and structural safety. Another issue associated with buildings within the tsunami inundation zone is to evaluate the design requirements for a structure to survive strong seismic ground shaking as well as subsequent tsunami forces. The design requirements for seismic response generally depend on structural flexibility, ductility and redundancy, while design for tsunami effects requires considerable strength and rigidity, particularly at the lower levels. These requirements need not be contradictory, but both must be considered.

These issues are particularly critical for buildings that may be used as evacuation shelters. In contrast to seismic ground shaking, there is usually a short lead-time prior to tsunami attack, which makes effective forewarning and evacuation possible. The lead-time can range from a few minutes for a local source to several hours for a distant source. Tsunami warning lead-times are shorter than those of many other natural hazards, e.g. volcanic eruptions, hurricanes, and floods. Hence, in some situations, vertical evacuation to upper floors or evacuation to tsunami resistant buildings, i.e. tsunami shelters, within tsunami inundation zones is the only choice for human survival.

Past field observations, also supported by the numerical simulations, show that there is much variability over, not only cross-shore but also short alongshore distances in tsunami energy and resulting damage to coastal structures. Local amplification of tsunami energy along the shore results from the influence of three-dimensional bathymetry and coastal topography. The bathymetry leads to wave refraction, diffraction, reflection, and resulting interference phenomena that cause both focusing and de-focusing of tsunami energy. These factors account for the observed alongshore variability of wave energy. Building destruction is often exacerbated by the impacts of water-born missiles (floating automobiles, lumber and other debris). Hence final evaluation of tsunami effects on an individual structure should be made using case-by-case analysis.

It is our understanding that the guidelines and standards should be used for the initial and preliminary evaluation only. Because of the substantial uncertainties with respect to the tsunami phenomena, the design tsunami itself cannot be estimated systematically even if the design earthquake were to be identified. No rational stochastic approach is possible due to insufficient data to support its probability.

I. Background

Very little guidance is provided by current structural design codes for loads specifically induced by tsunami effects on coastal structures; the established design codes focus mainly on loadings due to riverine floods and storm waves. There are significant differences in physical conditions between tsunami and other floods. For a typical tsunami, the water surface fluctuates near the shore with amplitude of several meters during a period of a few to tens of minutes. This timescale is intermediate between the hours to days typical of riverine floods, and the tens of seconds or less associated with cyclic loading of storm waves. This intermediate timescale makes tsunami behaviors and characteristics quite distinct from other coastal hazards, and the effects cannot be inferred from common knowledge or intuition. The time scale is long enough to allow tsunami to penetrate a great distance inland, while it is still short enough to make the tsunami flow highly transient. Rapid rise and fall of tsunami inundation appears to enhance scour around a building. A relatively short lead-time for warning and evacuation likely leaves unsecured potentially hazardous objects behind, e.g. propane gas cylinders, automobiles, and boats. These objects can cause devastating effects once they become water-borne missiles. With sufficient lead-time such as is the case with hurricane, the damage potential can be reduced by securing floatable (and/or flammable) objects, as well as by moving motor vehicles inland. For tsunami events, extended runup durations introduce the potential to transport floating bodies (e.g. automobiles and driftwood) far inland, impacting buildings in their path.

In comparison to the case of riverine flooding, tsunami inundation fluctuates faster, hence there is a higher potential to cause greater buoyant forces to be exerted on buildings; i.e. the water level outside may increase rapidly while the inside is still dry and empty. Rapid water-level fluctuations induce pore-pressure gradients in the soil, which may loosen the foundation – in some cases the soil can be liquefied.

II. Tsunami Runup Behavior

Tsunami characteristics and behaviors in the runup zone are fundamentally unpredictable because they are highly influenced by the type of tsunami and the surrounding topography and bathymetry. The following qualitative descriptions are based on past observations.

- When a "very" long tsunami attacks land on a steep slope, its runup can be characterized as a gradual rise and fall of water with no wave breaking. The 1960 Chilean tsunami at several Japanese towns and the 1964 Alaska tsunami at the town of Port Alberni, Canada, are classic examples. Figure 1 shows this type of tsunami runup, which was recorded at the 1983 Japan Sea Tsunami, and the effect in Port Alberni, which is shown in Fig. 2.

- Tsunamis often break offshore, forming a broken wave (bore) propagating near the shore as shown in Fig. 3. The subsequent runup from the bore is often termed "surging." The runup conditions recorded at several locations during the 1983 Japan Sea Tsunami are examples: see Fig. 4. A highly turbulent tsunami tongue sweeps the land.

- While the runup zone is flooded by a previous tsunami, the subsequent tsunami could impact buildings with the formation of a bore. A series of breaking waves riding on a long wave was recorded for the 1983 Japan Sea Tsunami. When the area has be inundated by a previous wave, a bore formation in the inland runup zone is possible.

- It appears that the total destruction of Scotch Cap Lighthouse (Fig. 5), Unimak Island, by the 1946 Aleutian tsunami must have resulted from a wave breaking directly onto the structure. This condition could be equivalent to a "collapsing" breaker, one of the classifications of wave breakers used in the field of coastal engineering (Weigel, 1964). This classification must be limited to the region very close to the shoreline with a steep-slope beach. A collapsing breaker observed in a laboratory is shown in Fig. 6.
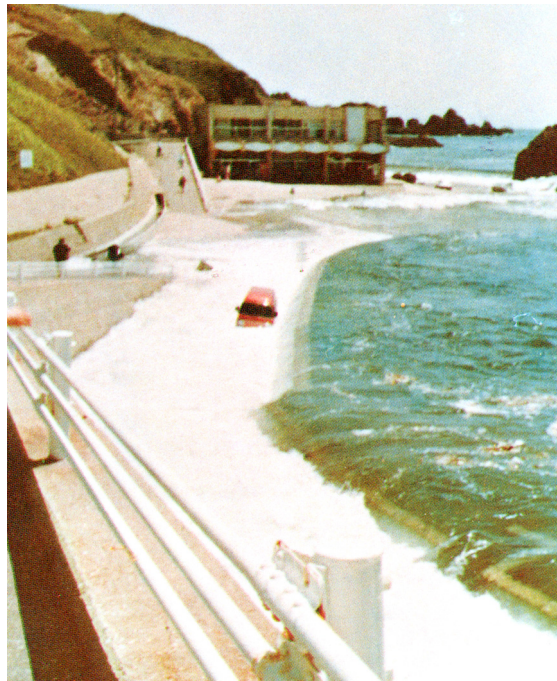
Fig. 1. Ojika Aquarium (Photo by S. Sato; In Tsunami Prevention Laboratory Research Report No. 1, 267 pp.)

Fig. 2. A scene of the 1964 Alaska Tsunami at Port Alberni, BC, Canada. (Photo by D. H. Peregrine)

Fig. 3. Bore formation of tsunami at Yatsumori during the 1983 Japan Sea Tsunami (Photo by N. Sasaki; In Tsunami Prevention Laboratory Research Report No. 1, 267 pp.)

Fig. 4. Iwaki River (Photo by N. Nara; In Tsunami Prevention Laboratory Research Report No. 1, 267)

Fig. 5. Scotch Cap Lighthouse destroyed by the 1946 Aleutian Tsunami.
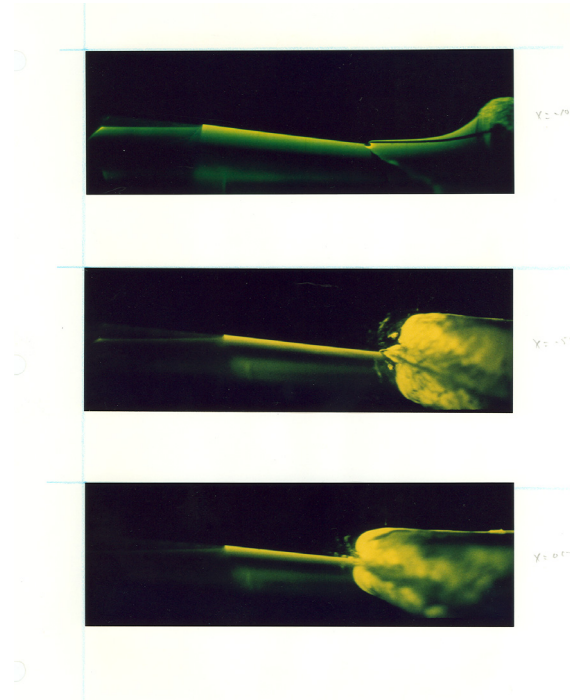
Fig. 6. A collapsing breaker resulted from an undular bore. (Yeh, et al. 1989)

III. Empirical Data

Shuto (1994) summarized the degrees of building damage as shown in Fig. 7; the marks filled in black are the data from the 1993 Okushiri Tsunami, and the open marks are those from previous events. Although no detailed information (e.g. the building locations and flow velocities) is given and the tsunami heights in the figure are the values of the maximum runup heights in the vicinity of the buildings, Shuto's data clearly indicate that reinforced concrete buildings can withstand a majority of tsunami attacks: the exception is the total destruction of Scotch Cap Lighthouse as shown in Fig. 5. Using generalized estimates as their basis, Matsutomi and Shuto (1994) presented guidance to building type survival in terms of the local tsunami flow speed as shown in Table 1. Note that the forces in the table are presented in tons-force per unit breadth in meter.
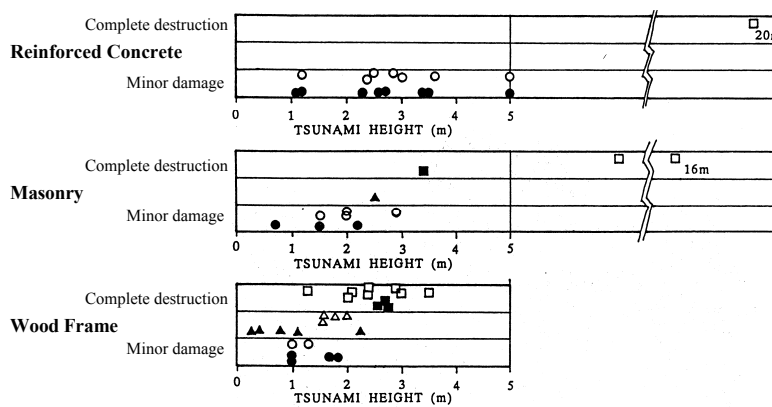
Fig. 7. Degrees of building damage v.s. tsunami runup height. The marks filled in black are the data from the 1993 Okushiri tsunami; the hollow marks are the data from the previous tsunami events. (Shuto, 1994)

5

Table 1: Building type survival in terms of the local tsunami flow speed (Matsutomin and Shuto, 1994)

Type of building	Flow velocity (m/s)	Forces (tf/m)
Reinforced concrete	> 10.2	> 16.9
Masonry	10.2	16.9
Wood Frame	4.2	1.06

IV. Current Design Code Loads

The design codes reviewed for this study provide guidelines and equations for loads that would be expected on a structure in flood and wave situations. The relevant codes available at present are:

- The City and County of Honolulu Building Code (CCH) Chapter 16 Article 11 authored by Department of Planning and Permitting of Honolulu, Hawaii, contains information on regulations that apply within flood hazard districts and for developments adjacent to drainage facilities. The loading requirements are based on equations from Dames & Moore, 1980.

- The 1997 Uniform Building Code (UBC 97) Appendix Chapter 31 authored by the International Conference of Building Officials (ICBO) covers special construction topics in flood resistant construction.

- The 2000 International Building Code (IBC 2000) authored by the International Code Council provides information on flood design and flood resistant construction in Appendix G.

- The ASCE 7-98 (ASCE 7) authored by American Society of Civil Engineers Committee 7 describes the different forces involved with flood and wave loads.

- The Federal Emergency Management Agency Coastal Construction Manual (FEMA CCM) contains expressions for flood loads which include wave loads.

The scope of the codes indicates that within flood hazard areas, all new construction including structures and portions of buildings and structures, as well as substantial improvements and restoration of damage to buildings and structures, be designed and constructed to resist the effects of flood hazards and flood loads. The base flood elevation shown on an approved flood hazard map is the minimum elevation used to define areas prone to flooding, unless records indicate a higher elevation should be used. It should be noted that all of the codes assume that jurisdictions are participating in the National Flood Insurance Program (NFIP). All referenced codes provide the same definition of flood hazard zones because they are based on the NFIP. Areas that are prone to flooding but not subject to wave heights of more than 3 feet (~ 1 m) are designated as A zones. The codes classify areas that have wave heights in excess of 3 feet (~ 1 m) or subject to high-velocity wave run-up or wave-induced erosion as coastal high-hazard zones or V zones.

In coastal floodwater design, buildings or structures should be designed to resist the effects of coastal floodwaters and tsunamis. Flood-proofing methods must be adequate to resist the flood depths, pressures, velocities, impact, uplift forces, and other factors associated with the flood, including floodwaters due to tsunamis in coastal high hazard districts. Habitable space in the building must be elevated above the regulatory flood elevation by such means as posts, piles, piers or shear walls parallel to the expected direction of flow of the tsunami wave. The forces

and effects of floodwaters on the structure are to be accounted for in the design. The following loads must be considered in the design and construction of buildings and structures in V zones: hydrostatic (vertical and lateral), hydrodynamic, impact, surge, wave and breaking wave loads. Spaces below the design flood elevation must be free from obstruction. Non-structural walls below the design flood elevation must be designed to break away during flooding or tsunami inundation. The effects of long-term erosion, storm-induced erosion and local scour are to be included in the design of foundations of buildings or other structures in coastal high hazard areas. Foundation embedment should be below the depth of potential scour. All buildings and structures in potential flood zones must be designed and constructed to resist flotation from floodwater at the regulatory flood elevation. Allowable stresses or load factors in the case of ultimate strength or limit design for the building materials used shall be the same as the building code provides for wind or earthquake loads combined with gravity loads, i.e., loads and stresses due to tsunamis are to be treated in the same fashion as for earthquake loading.

- **Hydrostatic Forces**
  - Hydrostatic forces occur when standing or slowly moving water encounters a building or building component. Hydrostatic loads can act laterally on an object. This load always acts perpendicular to the surface to which it is applied. It is caused by an imbalance of pressure due to a differential water depth on opposite sides of a structure or structural member.

- **Buoyant Forces**
  - The buoyant or vertical hydrostatic forces on a structure or structural member subject to partial or total submergence will act vertically through the center of mass of the displaced volume. Buoyant forces are a concern for basements, empty above-ground and below-ground tanks, and for swimming pools. Any buoyant force on an object must be resisted by the weight of the object and any opposing force resisting flotation.

- **Hydrodynamic Forces**
  - When water flows around a building (or structural element or other object) hydrodynamic loads are applied to the building. These loads are a function of flow velocity and structure geometry, and include frontal impact on the upstream face, drag along the sides, and suction on the downstream side. These loads are induced by the flow of water moving at moderate to high velocity. They are usually called the drag forces, which are combination of the lateral loads caused by the impact of the moving mass of water and the friction forces as the water flows around the obstruction.

- **Surge Forces**
  - Surge forces are caused by the leading edge of a surge of water impinging on a structure. The surge force is computed as a force per unit width on a vertical wall subjected to a surge from the leading edge of a tsunami.

- **Impact Forces**
  - Impact loads are those that result from debris such as driftwood, small boats, portions of houses, etc., or any object transported by floodwaters, striking against buildings and structures or parts thereof. The magnitude of these loads is very difficult to predict, yet some reasonable allowance must be made for them. The velocity of waterborne objects are assumed to be the same as the flood velocity. The object is assumed to be at or near

the water surface level when it strikes the building. Therefore, the object is assumed to strike the building at the water level. Uncertainty about the duration of the impact time is the most likely cause of error in the calculation of debris impact loads. According to Chopra (1995), the duration of impact is influenced primarily by the natural frequency of the building, which is a function of the building's "stiffness." This stiffness is determined by the properties of the material being struck by the object, the number of supporting members (columns or piles), the height of the building above the ground, and the height at which the building is struck.

- **Breaking Wave Forces**
  - Two breaking wave load conditions are of interest in construction; waves breaking on small-diameter vertical elements (e.g., piles, columns in the foundation of a building in V zones) and waves breaking against walls (e.g., breakaway walls in V zones). Breaking wave forces are modified in instances where the walls or surfaces upon which the breaking waves act are non-vertical. Breaking waves that are obliquely incident and not perpendicular to the wall result in a lower force. The net force resulting from breaking wave acting on a rigid vertical pile or column is assumed to act at the still water elevation. A wave breaking against a vertical wall causes a reflected or standing wave to form against the seaward side of the wall. The crest of the wave is some height above the still water elevation. Two cases are considered: (1) where a wave breaks against a vertical wall of an enclosed dry space, and (2) where the still water level on both sides of the wall is equal. Case 1 is equivalent to a wave breaking against an enclosure in which there is no floodwater below the still water level. Case 2 is equivalent to a wave breaking against a wall with openings that allow floodwaters to equalize on both sides of the wall.

The estimation of design flood velocities in coastal flood hazard areas is subject to considerable uncertainty. There is little reliable historical information concerning the velocity of floodwaters during coastal flooding. The direction and velocity of floodwaters can vary significantly throughout a coastal flood event. In a similar manner, flow velocities can vary from close to zero to high velocities during a single flood. For these reasons, flood velocities should be estimated conservatively by assuming floodwaters would approach from the most critical direction and by assuming high flow velocities. Tsunami modeling of potential tsunami effects on a specific location could be used to determine a design flow velocity. Current codes do not mention the potential of site-specific tsunami modeling.

IV-a. Design Code Equations

Based on a comparison of the individual code equations, a set of generalized expressions for wave and flood loads on a structure are presented. These include generalized equations for hydrostatic force, buoyant force, hydrodynamic force, surge force, impact force, breaking wave forces and design flood velocity.

Hydrostatic Force
The CCH and FEMA CCM provide similar expressions for lateral hydrostatic force. The CCH equation includes a velocity head while the FEMA CCM does not include the velocity head. The CCH equation was selected because it is somewhat more conservative. It has been noted (Dames and Moore, 1980) that hydrostatic forces are normally relatively small compared to surge and drag forces for the case of bore-like tsunamis, however for tsunamis that act as a rapidly rising

tide, the hydrostatic forces generally become increasingly important. This equation does not include the direct drag at the top of a wall when the wall is less than h in height.

$$F_h = \frac{1}{2}\rho g \left(h + \frac{u_p^2}{2g} \right)^2,$$ (1)

where F_h is the hydrostatic force on a wall, per unit width of wall, ρ is the water density, g is the gravitational acceleration, h is the water depth, and u_p is the velocity component normal to the wall. The resultant force will act horizontally at a distance of h_R above the base of the wall where:

$$h_R = \frac{1}{3}\left(h + \frac{u_p^2}{2g} \right).$$ (2)

Buoyant Force

All codes provided the same expression for buoyant force, F_b:

$$F_b = \rho g V,$$ (3)

where V is the volume of water displaced by the building.

Design Flood Velocity

FEMA CCM and CCH provide the following estimate of the flood velocity u in the surge depth d_s, based on Dames & Moore (1980):

$$u = 2\sqrt{gd_s}.$$ (4)

Hydrodynamic Force

Both CCH and FEMA CCM provide the following expression for hydrodynamic force (drag force) F_d:

$$F_d = \frac{1}{2}\rho C_d A u_p^2,$$ (5)

where C_d is the drag coefficient, and A is the projected area of the body on the plane normal to the flow direction. The CCH recommends $C_d = 1.0$ for circular piles, 2.0 for square piles and 1.5 for wall sections. The FEMA CCM recommends $C_d = 2.0$ for square or rectangular piles and 1.2 for round piles. In addition, Table 2 is given for the drag coefficients for larger obstructions.

Surge Force

The CCH adopted the following equation (Dames & Moore, 1980) for surge force F_s.

$$F_s = 4.5\rho g h^2,$$ (6)

where h is the surge height. The resultant force acts at a distance approximately h above the base of the wall. This equation is applicable for walls with heights equal to or greater than $3h$. Walls whose heights are less than $3h$ require surge forces to be calculated using appropriate combination of hydrostatic and hydrodynamic force equations for the given situation.

Table 2: The drag coefficient recommended by FEMA CCM.

Width to Depth Ratio (w/ds or w/h)	Drag Coefficient C_d
From 1 - 12	1.25
13 - 20	1.3
21 - 32	1.4
33 - 40	1.5
41 - 80	1.75
81 - 120	1.8
> 120	2

Impact Force

The CCH, FEMA CCM and ASCE 7 contained similar equations that resulted in the following generalized expression for impact force F_I acting at the still water level:

$$F_I = m\frac{du_b}{dt} = m\frac{u_I}{\Delta t},$$ (7)

where u_b is the velocity of the impacting body, u_I is its approach velocity that is assumed equal to the flow velocity, m is the mass of the body, Δt is the impact duration that is equal to the time between the initial contact of the body with the building and the maximum impact force. The CCH recommends Δt values for wood construction as 1.0 second, steel construction as 0.5 second, and reinforced concrete as 0.1 second. The FEMA CCM provides the Δt values shown in Table 3.

Table 3: The impact duration recommended by FEMA CCM.

Type of construction	Duration (t) of Impact (sec)	
	Wall	**Pile**
Wood	0.7 - 1.1	0.5 - 1.0
Steel	NA	0.2 - 0.4
Reinforced Concrete	0.2 - 0.4	0.3 - 0.6
Concrete Masonry	0.3 - 0.6	0.3 - 0.6

Breaking Wave Forces

Breaking Wave Loads on Vertical Piling and Columns

The ASCE 7 and FEMA CCM provide the following expression for the breaking-wave force F_{brkp}:

$$F_{brkp} = \frac{1}{2}\rho g C_{db} D H_b^2,$$ (8)

where C_{db} is a shape coefficient (ASCE 7 and FEMA CCM recommended C_{db} values of 2.25 for square or rectangular piles and 1.75 for round piles), D is the pile diameter, and H_b is the breaking wave height –(FEMA CCM recommends that $H_b = 0.78\, d_s$ in which d_s is the design still-water flood depth).

Breaking Wave Loads on Vertical Walls

Equations from both FEMA CCM and ASCE 7 are given because their equations differ slightly so no generalized equation was determined. The following equations are from FEMA CCM, which incorporates the lateral hydrostatic force. If this formula is used then the hydrostatic force should not be added.

Case 1 (enclosed dry space behind wall):

$$f_{brkw} = 1.1C_p \gamma d_s^2 + 2.41 \gamma d_s^2. \tag{9}$$

Case 2 (equal still water level on both sides of wall):

$$f_{brkw} = 1.1C_p \gamma d_s^2 + 1.91 \gamma d_s^2, \tag{10}$$

where f_{brkw} is the total breaking wave load per unit length of wall acting at the still water level (d_s), C_p is the dynamic pressure coefficient from Table 4, and γ is the specific weight of water.

Table 4: The dynamic pressure coefficient recommended by FEMA CCM.

Cp	Building Type	Probability of Exceedance
1.6	Accessory structure, low hazard to human life or property in the event of failure	0.5
2.8	Coastal residential building	0.01
3.2	High-occupancy or critical facility	0.001

The following equations are provided by ASCE 7:

$$P_{max} = C_p \gamma d_s + 1.2 \gamma d_s, \tag{11}$$

$$F_t = 1.1C_p \gamma d_s^2 + 2.4 \gamma d_s^2, \tag{12}$$

where P_{max} is the maximum combined dynamic ($C_p \gamma d_s$) and static ($1.2\gamma d_s$) wave pressure, also referred to as shock pressure, and F_t is the total breaking wave force per unit length of the structure, also referred to as shock, impulse or wave impact force acting near the still water elevation (d_s). C_p is the dynamic pressure coefficient ($1.6 < C_p < 3.5$: see Table 5), and d_s is the still water depth at base of building where the wave breaks. If free water exists behind the wall, the hydrostatic component of the wave pressure and force disappears and the dynamic wave pressure and the net force are computed by:

$$P_{max} = C_p \gamma d_s \tag{13}$$

$$F_t = 1.1C_p \gamma d_s^2 \tag{14}$$

Table 5: The dynamic pressure coefficient recommended by ASCE 7. Building category: I, low hazard; II, standard; III, substantial hazard; IV, essential facilities.

Building Category	Cp
I	1.6
II	2.8
III	3.2
IV	3.5

Table 6 (from ASCE 7)

Name of Occupancy	Category

Structures that represent a low hazard to human life in the event of failure including, but not limited to:
    agricultural facilities
    certain temporary facilities
    minor storage facilities
	I

All structures except those listed in Categories I, III and IV	II

Structures that represent a substantial hazard to human life in the event of failure including, but not limited to:
    Structures where more than 300 people congregate in one area
    Structures with elementary school, secondary school, or day-care facilities with capacity greater than 250
    Structures with a capacity greater than 500 for colleges or adult education facilities
    Healthcare facilities with a capacity of 50 or more resident patients but not having surgery or emergency treatment facilities
    Jails and detention facilities
    Power generating stations and other public utility facilities not included in Category IV
    Structures containing sufficient quantities of toxic or explosive substances to be dangerous to public if released
	III

Structures designated as essential facilities including but not limited to:
    Hospitals and other health-care facilities having surgery or emergency treatment facilities
    Fire, rescue, and police stations and emergency vehicle garages
    Designated earthquake, hurricane, or other emergency shelters
    Communications centers and other facilities required for emergency response
    Power generating stations and other public utility facilities required in an emergency
    Structures having critical national defense functions
	IV

Loading Combinations

Individual loading conditions must be applied to standard elements in appropriate load combinations. The following load combinations are by FEMA CCM, based on Dames & Moore, 1980. The structural members considered in these references are piles or open foundations, columns, walls and basements. Outer edge beams at second floor level are not mentioned because the reference codes are intended for smaller scale residential structures.

Type 1 -- Columns in tsunami prone areas (Required):
    The following combinations are used to calculate the force on a column from a tsunami with the additional impact force from debris.

$$F_{brkp} \text{ (on column)} + F_i \text{ (on column), or } F_d \text{ (on column)} + F_i \text{ (on column).}$$

Type 2 -- Solid walls facing the shoreline in tsunami prone areas:
    Construction of non-breakaway walls or solid walls parallel to the shorelines is not recommended in structural designs. The combinations provided below are for walls, which are perpendicular to the flow of the tsunami.
    Tsunami effects on structural walls with additional impact force of debris.

$$F_{brkw} \text{ (on walls facing shoreline)} + F_i \text{ (on one corner) or}$$

$$F_s \text{ (on walls facing shoreline)} + F_i \text{ (on one corner) or}$$

$$F_d \text{ (on walls facing shoreline)} + F_i \text{ (on one corner).}$$

Type 3 -- Vertical (Buoyant) Forces on Structure:
    This loading combination is used when there is a sudden increase in the water level. The buoyant force on the structure must also be considered with other lateral forces.

$$F_b \text{ (for basements, swimming pools, empty above-ground and below ground tanks).}$$

Breakaway walls

The design codes specify that all non-structural walls below the anticipated flow depth be designed as breakaway walls. These walls and their connections are required to be designed for a lateral pressure not less than 10 psf and not more than 20 psf.

Scour

The codes indicate that the potential for scour around structural foundations must be considered, but provide no guidance on how this scour can be estimated or how footings can be designed to withstand the effects of scour.

<div align="center">

IV-b. Comments

</div>

All of the equations presented above appear reasonable and might be applicable to tsunami cases. Nonetheless, the following comments can be made based on recent analysis of tsunami runup.

- Equation (1) – the representation of hydrostatic force – may not be relevant to a building with a finite breadth, for which the water can flow around and quickly fill up behind the building. Hydrostatic force is usually important for a 2-D structure such as seawalls and dikes or for evaluation of an individual wall panel where the water level outside differs substantially from the level inside.

- The surge-speed estimate (4) may be too crude. This equation was suggested by Camfield (1980). The speed evaluated by (4) is equivalent to a classic solution of the leading-tip of surge on a frictionless horizontal plane generated by breaking a dam with the quiescent impoundment depth of d_s. Hence the computed tip velocity does not represent the velocity of a flow depth d_s, and therefore this equation is not appropriate to represent the flow velocity for a tsunami flood passing through a structure.

- The surge-force computation by (6) may result in excessively overestimated values. Note that (6) was derived by summing the hydrostatic force and the change in linear momentum at the impingement of a surge front on a vertical wall. The surge impingement is treated as steady using the speed evaluated by (4). The estimation made by (6) implies that the surging force would be 9 times the hydrostatic force alone. As discussed later, such an excessively large surging force is contradictory to the laboratory results by Ramsden (1993) and Arnason (2005).

- The present investigation focuses on construction and evaluation of tsunami shelters and engineered multistory buildings that may be used for vertical evacuation. These buildings and shelters are usually constructed on land some distance from the shoreline. Hence, wave-breaking force exerting directly onto the shelter would be a rare case, unless a building, such as the lighthouse at Scotch Cap, is located right at the shoreline (see. Fig. 5).

- Present guidelines for the loading combinations needs careful consideration for further improvement.

V. Factors to consider when designing a tsunami shelter

For a specific site, the following factors must be considered for a tsunami resistant building and/or tsunami shelter design. First, the shelter must be able to withstand seismic ground shaking

that often precedes the tsunami attack: note that seismic ground shaking and tsunami attack are seldom concurrent. Tsunami shelters located near the shore must be evaluated both for resistance to structural failure and foundation failure resulting from soil liquefaction and/or scour. Second, the shelter must provide sufficient floor space for the evacuees above the base flood elevation. No matter how strong the shelter is, the evacuees may drown if the shelter is submerged by the inundation. Third, the shelter must withstand tsunami-induced forces, including impacts of water-borne missiles. Tsunamis often trigger fires; hence the shelter must be fire resistant. Lastly, careful attention must be paid to evaluation of tsunami-induced scour around the shelter's foundation. The rapid increase and recession of water level may loosen the soil skeleton, enhancing scour, possibly destabilizing the structure.

Flood and wave forces discussed in Section IV are categorized in Table 7. All of the forces are relevant for tsunamis as well, although some are more important than the others. Evaluation of each force requires the flow depth and velocity. Hence we must first establish a rational methodology for determining these parameters.

Table 7: Considerations for tsunami forces.

Type of forces	Comments for tsunami considerations
Hydrostatic Forces	Not used for the evaluation of a building as a whole, but need to be consider for the strength of each structural wall panel of the building.
Buoyant Forces	Controlled by the inundation depth and the rate of water-level increase
Hydrodynamic Forces	Controlled by the maximum value of the product of the inundation depth, the square of flow velocity, and the shape of the structural element.
Surge Forces	Controlled by the flow velocity of the leading tongue of the runup
Impact Forces	Controlled by the maximum flow velocity and depth, object mass, and elasticity associated with the impact.
Breaking Wave Forces	May not be relevant to the tsunami forces on onshore buildings: Tsunami waves tend to break offshore and approach the shore as a broken bore.
Scour	Controlled by flow velocity (shear stress), and pore-pressure gradient that can be estimated by the change in inundation depth and its duration.

Tsunami Runup

To predict the flow velocities and depths for a given design tsunami at a site of interest, the best practice available is to run a detailed numerical simulation model with a very fine grid size in the runup zone. Usually such a numerical model is run with the nested grid system: running with a grid size of several kilometers in the abyssal plain, a few hundreds of meters on the continental shelf, a few tens of meters near the shore and a smaller grid size for the runup zone. The numerical simulation can provide the complete time history of flow velocity and depth at the site of interest. Drawbacks of this approach are that 1) such a simulation model is not readily available to the public and requires significant resources (time, money, and expertise), and 2) the

results – in particular the flow velocities – may not be as accurate as expected, depending on the mesh size and the runup algorithm.

Alternatively, the use of analytical solutions should be considered. While some simplifications and assumptions must be imposed onto the analytical solutions, the results are useful as guidelines. The available analytical solutions are based on the one-dimensional fully nonlinear shallow-water-wave theory for the condition with a uniformly sloping beach. With these assumptions, the exact solution for the runup resulting from an incident uniform bore was given by Ho and Meyer (1962). The maximum runup velocity occurs at the leading tip and was found to be:

$$\frac{u}{\sqrt{2\ell g \alpha}} = \sqrt{1 - \frac{x}{\ell}} \,, \tag{15}$$

where ℓ is the total runup distance (from the initial shoreline to the maximum runup), α is the beach slope, g is the gravitational acceleration, and x measures inshore distance from the initial shoreline to the location of interest. Furthermore, the exact solution algorithm for non-breaking tsunamis of the general initial forms was recently developed by Carrier et al. (2003). Using this algorithm, Yeh (2005) plotted the envelope curves of the maximum momentum flux per unit water mass hu^2 as shown in Fig. 8. In this figure, the numerical result for uniform-bore runup is also plotted and presented in red. The plots in Fig. 8 yield the algebraic representation of the envelop of the maximum momentum flux per unit water mass hu^2:

$$\frac{hu^2}{g\alpha^2\ell^2} = 0.11\left(\frac{x}{\ell}\right)^2 + 0.015\left(\frac{x}{\ell}\right). \tag{16}$$
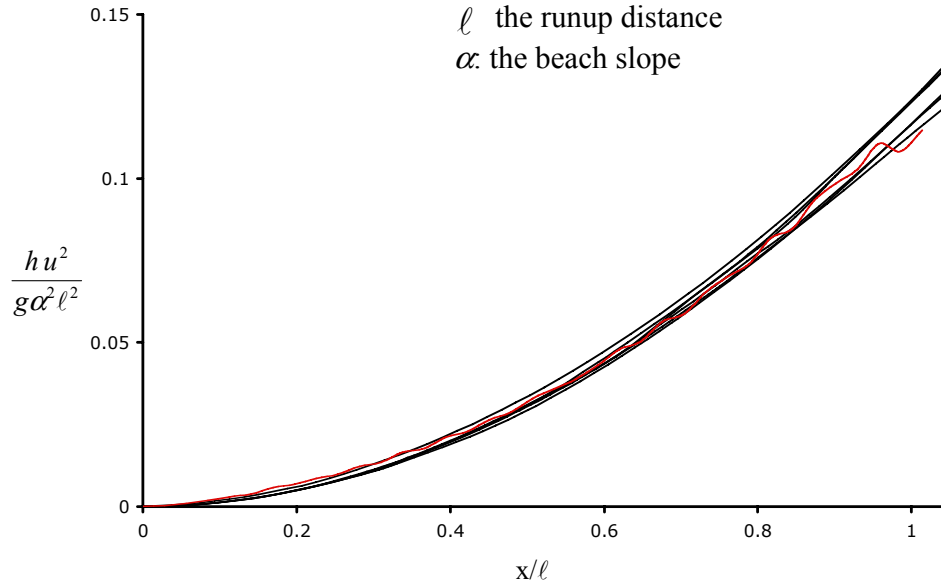
Fig. 8. Linear momentum flux per unit mass for 1-D tsunami runup. Analytical solution for non-breaking tsunami in black (Carrier et al. 2003) and numerical solution for bore runup in red.

15

Hence once the maximum runup distance is determined (perhaps from the available inundation map) for a given "uniform" beach slope, the maximum velocity at a given location x can be computed by (15) and the momentum flux $\rho\,h\,u^2$ by (16). The maximum inundation depth at a site of interest should be evaluated by the difference between the site elevation and the water-surface elevation at the maximum runup location, which is the limited condition for a very long wave. Although a real beach is not uniformly sloped nor is tsunami runup one-dimensional motion, (15) and (16) will provide the analytical basis for the runup conditions. It must be noted that Fig. 8 and (16) were obtained by evaluating a variety of cases with the algorithm given by Carrier et al. (2003) plus the numerical evaluation of bore runup (George, 2004), and is currently being reviewed for publication (Yeh, 2005).

Hydrostatic Force

Hydrostatic forces can be considered not dominant for tsunami, unless a subject structure is very wide (e.g. sea wall) so that the space behind it remains dry. Hence for buildings with breakaway walls on the ground level, this force is irrelevant.

Buoyant Force

Because of the rapid increase in water level, the buoyant effect induced by a tsunami may be more important than for the cases of riverine flood. Figure 9 shows a house that was floated and transported some distance during the 1994 South Kuril Island Tsunami in Kunashir Island, Russia/Japan. This force must be considered in conjunction with other relevant lateral forces. We therefore propose that the maximum inundation depth should be used for the evaluation in (3); which assumes that the inside of the building remains completely dry. Note that if the exterior walls are designed as breakaway walls, this will substantially reduce the likely uplift due to the buoyant force.

Fig. 9. At Yuzhokurilsk, Kunashir Island, during the 1994 Shikotan Tsunami, this house drifted 300 m inshore along the river bed.

16

Hydrodynamic Force (Drag Force)

This force can be computed by (5) and (16): note that the projected area *A* in (5) is the product of the flow depth *h* and the breadth of the structural element being considered. For a given location, the design value of $h\,u^2$ can be computed by (16), and the hydrodynamic force can be evaluated by (5). The drag coefficient C_D for a square shaped column is approximately 2 based on the laboratory experiments by Arnason (2005) as shown in Fig. 10; the value $C_D = 2$ is comparable to those listed in the present codes (see Table 2). Note that Arnason's experiments apply only to a bore impinging onto a column. The bore was generated by lifting a vertical gate, which initially separates the impounded water from a very thin sheet of water (2 cm) in front of the gate. The overshoot seen in Fig. 10 at the initial impingement can be interpreted as the "surging" force, which we describe next.
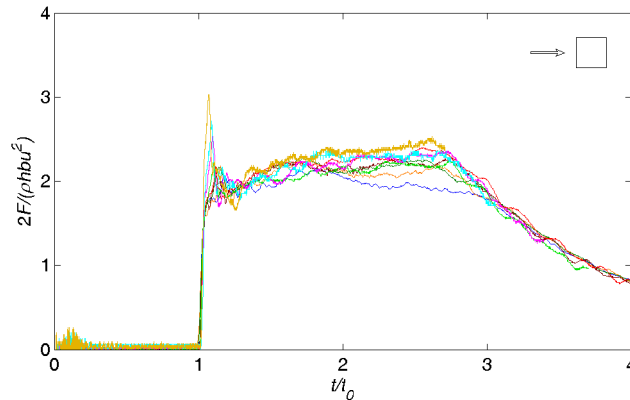
Fig. 10. Laboratory data of hydrodynamic tsunami force on a squire column: C_d (Arnason, 2004)

Surging Force

As we discussed in Sec. IV-b, the surging force computed by (6) may be inadequate, which results in significant overestimation. Figure 10 shows that the maximum surging force that Arnason (2005) obtained in his experiments was $1.5\,\rho A u^2$, which is equivalent to $C_D = 3$ in (5). Arnason's data indicate that the value of "surging" C_D increases when the ratio of the surge height to the column width reduces.

Ramsden (1993) performed comprehensive experiments on surging forces on a vertical wall in a narrow wave flume: the condition is equivalent to the vertical wall of infinite breadth. Figure 11 shows a comparison between the impact of a strong turbulent bore and a dry bed surge. Figure 11-d shows no initial impact force (so-called "surging" force) for the case of the dry-bed surge, while a clear overshoot for the case of the bore is observed at approximately 0.7 sec after the initial contact to the wall. Also note that the overshoot in the bore case is approximately 1.5 times the subsequent hydrodynamic force, which is consistent with Arnason's (2005) results in Fig. 10. The lack of the overshoot may be attributed to the relatively mild-slope front profile of the dry-bed surge as shown in Fig. 11-a: the impact momentum increases gradually in comparison with the sudden slam of the steep front in the case of the turbulent bore. Since the turbulent bore loading is greater than that generated by a dry-bed surge, the surge loading may be ignored in the design guideline.
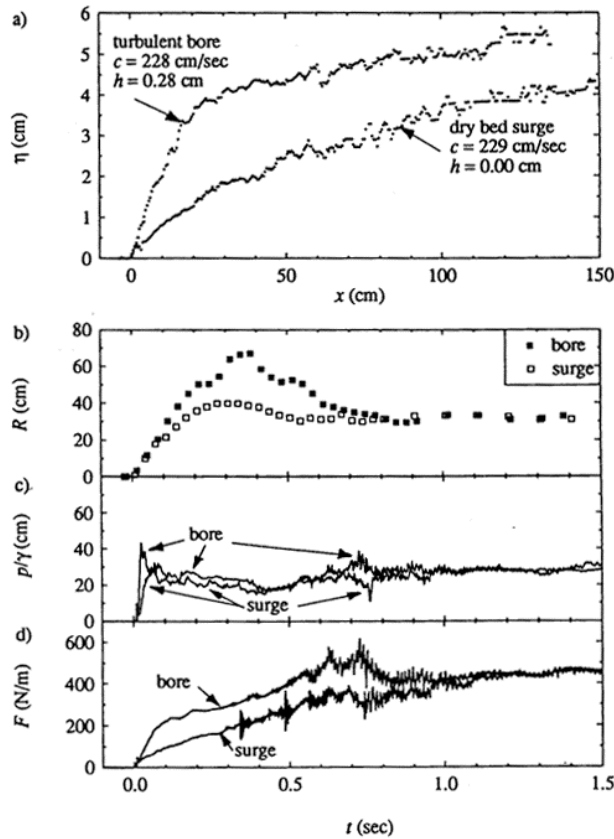
Fig. 11. Comparison of the experimental a) wave profile; b) runup; c) pressure head; and d) force due to a strong turbulent bore and a dry bed surge (after Ramsden, 1993)

Impact Force

The impact force of a water-borne missile (floating automobiles, buildings, drift wood, lumber, etc.) can be the dominant cause for building destruction. Unfortunately, it is difficult to estimate this force accurately. The recommended equation in the present codes (7) is based on the concept of the impulse-momentum approach: the impulse of the resultant force acting for an infinitesimal time is equal to the change in linear momentum. For the actual computation, a small-but-finite time Δt (not infinitesimal) and the averaged change in momentum are used as the approximations. As seen in (7), it contains significant uncertainty in evaluating the duration of impact, Δt.

The impulsive forces of driftwood were investigated experimentally by Matsutomi (1999). He performed two sets of experiments: one in a small water tank and the other for full-scale impact in air. In his small water tank, a bore (and a surge) was generated by lifting the partition gate, just as in Arnason's (2005) experiments. A scaled-down driftwood model was placed 2.5 m upstream from the receiving wall. The model driftwood was picked up by the generated bore (or surge), and impacted onto the vertical wall. Based on his regression analysis with a large amount of data, Matsutomi proposed the following empirical equation for the impact force F:

$$\frac{F}{\gamma_w D^2 L} = 1.6 C_M \left(\frac{u}{\sqrt{gD}} \right)^{1.2} \left(\frac{\sigma_f}{\gamma_w L} \right)^{0.4},$$

(17)

where γ_ω is the specific weight of the wood, D and L are the diameter and the length of the wood, C_M is a coefficient that depends on the flow passing around the receiving wall, u is the velocity of the wood at impact, and σ_f is the yield stress of the wood. Matstutomi recommended the use of $\sigma_f = 20$ MPa for wet lumber. From his experimental data, he recommends the value of $C_M \approx$ 1.7 for a bore or surging condition, and $C_M \approx 1.9$ for a steady flow. Based on (17), Matsutomi presented the design charts shown in Fig. 12.

Bores and Surges   Steady Flows
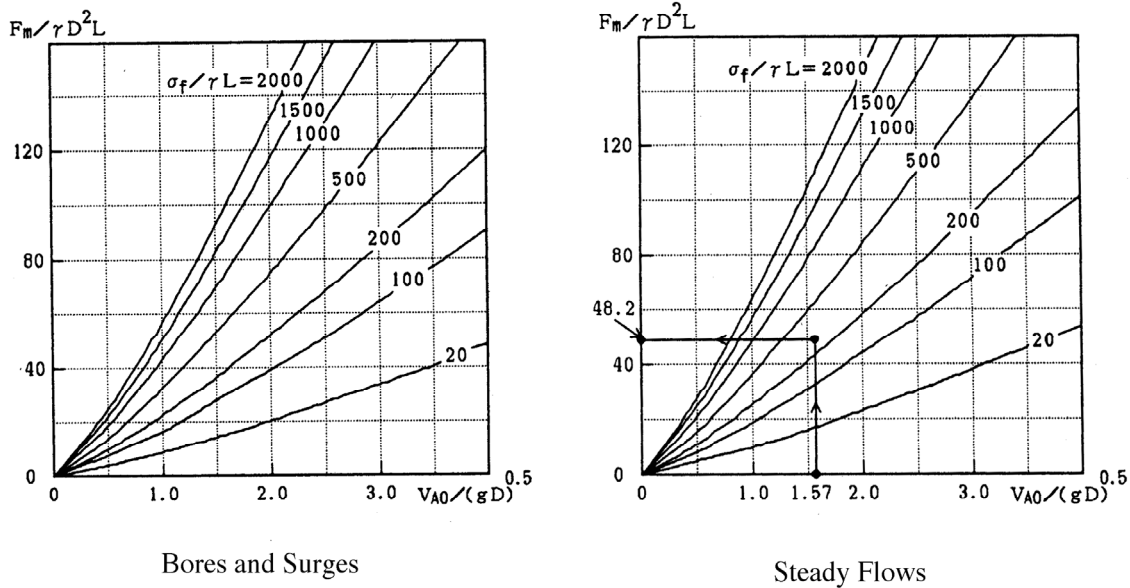
Figure 12. Impact forces of lumber (after Matsutomi, 1999)

Haehnel and Daly (2002) performed similar experiments to Matsutomi. They considered reduced scale logs in "steady" flow in a small flume, and prototype logs in a large towing basin (not in air, as in Matsutomi's experiments). Haehnel and Daly (2002) analyzed the data based on the one-degree-of-freedom model shown in Fig. 13. Since the collision occurs over a short duration, damping effects (ζ) are neglected. Furthermore assuming for a rigid structure that $k_S \gg k_t$ and k_l, the model can be formulated by:

$$m_1 \ddot{x} + \hat{k} x = 0, \tag{18}$$

where m_1 is the mass of the log, x is the summation of the compression of the building and the log during impact and rebound, the dot denotes the time derivative, and $\hat{k}$ is the effective constant stiffness associated with both the log and the building, i.e. $\dfrac{1}{\hat{k}} = \dfrac{1}{k_t} + \dfrac{1}{k_l}$. Solving (18) yields the maximum force to be:

$$F_{max} = Max.\langle \hat{k} x \rangle = u\sqrt{\hat{k} m_1}, \tag{19}$$

where u represents the impact velocity of the log. Based on their laboratory experiments, the effective constant stiffness, $\hat{k}$, between a log and a rigid building was estimated as 2.4 MN/m. It must be noted that their large-scale prototype experiments were performed in the towing basin, which means the log was not moving with the flow.

Haehnel and Daly (2002) suggest that the impulse-momentum approach can be reduced to the constant stiffness approach (19) by setting $\Delta t = \frac{\pi}{2}\sqrt{\frac{m_1}{\hat{k}}}$ (note that, to be consistent to (18), the force is a sinusoidal function in time), and the work-energy approach is also equivalent to (19) by setting the stopping distance $S = u\sqrt{\frac{m_1}{\hat{k}}}$.
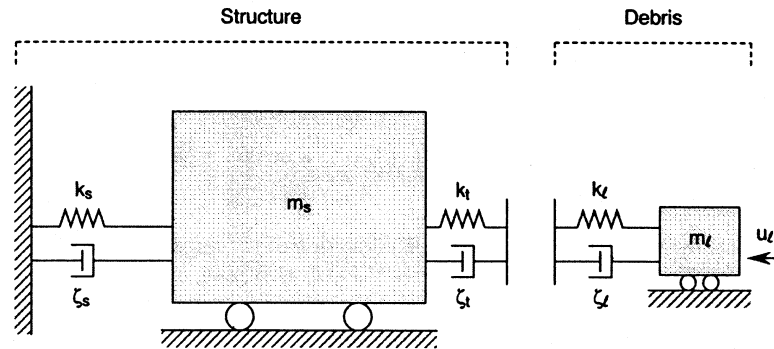
Figure 13. An impact model of a single debris element on a structure

It is emphasized that both Matsutomi (1999) and Haehnel and Daly (2002) assumed the effects of building flexibility to be unimportant and they therefore did not address this consideration. As far as a building used for a tsunami shelter is concerned, flexibility of the building itself should be unimportant, considering that it will likely be a relatively stiff reinforced concrete structure. Also note that errors associated with the use of a towing tank -- instead of the real condition of a log carried with flow -- may be significant in Haehnel and Daly's (2002) results. Matsutomi's (1999) correction factor C_M is intended to take into account this discrepancy.

Breaking Wave Forces

As we discussed earlier, it is very difficult to accurately estimate breaking wave forces. Considering a probable location of a tsunami shelter being sufficiently away from the shoreline, it is inconceivable that an incident tsunami will break directly onto the building; tsunami attack onto an inshore building will be in the form of a surge or turbulent bore. However, there are some buildings necessarily constructed very near the shoreline, for example a lighthouse. As discussed in Sec. II, the total destruction of the reinforced-concrete lighthouse at Scotch Cap, Unimak Island, probably resulted from a wave breaking directly onto the structure – see the rendering in Fig. 5. Careful and separate design considerations must be made for such special conditions.

Scour Effects

Tsunamis are known to cause substantial scour on shore. The scour mechanisms are expected to be different from those contributing to bridge or pier type scour processes in a river or offshore environment. The scouring associated with tsunami runup occurs over a short duration, less than half an hour, and no equilibrium state is reached. Tonkin et al. (2003) demonstrated in a series of scale model experiments that pore-pressure gradients developed in soils play a major role in scour. During the tsunami drawdown, the water level subsides and the pressure on the sediment

20

bed decreases, creating a vertical pressure gradient within the sand and decreasing the effective stress. Assuming that the surface pressure decreases approximately linearly from a sustained peak at ΔP to zero over time ΔT, Tonkin et al. (2003) combined the analytical solution with the soil stability condition given by the pore-pressure gradient and yielded the quantitative prediction for the movable soil depth, d_s, of tsunami-induced scour:

$$d_s = \frac{\Delta P}{\gamma_b \Lambda}\left(1 - 4\,\mathrm{i}^2\mathrm{erfc}\left[\frac{d_s}{2\sqrt{c_v \Delta T}}\right]\right) \qquad (20)$$

where Λ is the fraction of the buoyant weight of soil supported by the pore pressure gradient, γ_b is the buoyant specific weight of the saturated soil skeleton, c_v is the coefficient of consolidation, and $\mathrm{i}^2\mathrm{erfc}[\,\bullet\,]$ is the second integral of the complementary error function. Note that d_s is implicit in (20) and $\Lambda = 1$ represents zero effective stress condition at depth $= d_s$. Tonkin et al. (2003) suggested that $\Lambda \approx 0.5$ may be used to determine d_S by (20). The limiting condition of $d_S \rightarrow 0$ yields a measure of whether any soil instability due the pore-pressure gradient can occur:

$$\Lambda = \frac{2}{\sqrt{\pi}}\frac{\Delta P}{\gamma_b \sqrt{c_v \Delta T}}. \qquad (21)$$

The maximum scour effect should be evaluated both with the conventional steady flow approach (i.e. the function of shear velocity $u_* = \sqrt{\tau_0/\rho}$, τ_0 is the bed shear stress), and the enhancement caused by establishment of pore-pressure gradients (20).

VI. Summary

The following factors must be considered for tsunami shelter design. First, the shelter must be able to withstand seismic ground shaking that often precedes the tsunami attack: seismic ground shaking and tsunami attack are seldom concurrent. Tsunami shelters located near the shore must be evaluated both for resistance to structural and foundation failure. Second, the shelter must provide sufficient floor space for evacuees above the base flood elevation. No matter how strong the shelter is, evacuees may drown if the shelter is submerged by the inundation. Third, the shelter must withstand tsunami-induced forces, including impact of water-borne missiles. Tsunamis often trigger fires; hence the shelter must be fire resistant. Lastly, careful attention must be paid to evaluation of tsunami-induced scour around the shelter's foundation.

Based on the existing building codes together with recent literature review, we have identified potential forces that should be considered in establishing guidelines for tsunami-shelter design. All of the forces are relevant for tsunamis, although some are more important than others. Assuming that the tsunami shelters being constructed will be reinforced concrete or steel structures, and will be located in the tsunami inundation zone but inshore from the shoreline, the most probable forces will be the hydrodynamic force and the impact force. Once the flow depth and velocity at the shelter site are established, both forces can be computed in a rational manner with (5) and (17) or (19). Note that the present estimations of the impact force, (17) and (19), are not well established and need to be improved. To predict the flow velocities and depths for a given design tsunami at a site of interest, the best practice available is to run a detailed numerical simulation model with a very fine grid size in the runup zone.

References

American Concrete Institute. 1999. Building Code Requirements for Structural Concrete. ACI 318-99.

American Society of Civil Engineers. 1998a. Flood Resistant Design and Construction. ASCE Standard ASCE 24-98.

American Society of Civil Engineers. 1998b. Minimum Design Loads for Buildings and Other Structures. ASCE Standard ASCE 7-98.

Arnason, H. 2005. Interactions between and Incident Bore and a Free-Standing Coastal Structure, Ph.D. Thesis, University of Washington, Seattle, 172pp.

ASCE Standard. 2003. Minimum design loads for buildings and other structures. SEI/ASCE 7-02, 376 pp.

Bretschneider, Charles L. 1974. Development of Structural Standards in Flood and Tsunami Areas for the Island of Hawaii. Honolulu: Ocean Engineering Consultants, Inc. Prepared for Paul T. Taniguchi.

Camfield, F. (1980) "Tsunami Engineering," Coastal Engineering Research Center, US Army Corps of Engineers, Special Report (SR-6), 222 p.

Carrier, G.F., Wu, T.T. and Yeh, H. 2003. Tsunami Runup and Drawdown on a Plane Beach, Journal of Fluid Mechanics, 475, 79-99.

Dames & Moore. 1980. Design and Construction Standards for Residential Construction in Tsunami-Prone Areas in Hawaii. Prepared for the Federal Emergency Management Agency.

Department of Planning and Permitting of Honolulu Hawai'i. 2000. City and County of Honolulu Building Code. Chapter 16 Article 11. July.

Dudley, Walter C., and Min Lee. 1998. Tsunami. Honolulu: University of Hawai`i Press, Second Edition.

FEMA 2000. Coastal Construction Manual. FEMA 55, Federal Emergency Management Agency.

George, D. 2004. Personal communication.

Ghosh, S.K., and David A. Fanella (2003). Seismic and Wind Design of Concrete Buildings. Illinois: Country Club Hills.

Gonzalez, F.I. 1999. Tsunami! Scientific American, 280, 56-65.

Haehnel, R.B., and Daly, S.F. 2002. Maximum impact force of woody debris on floodplain structures. Technical Report: ERDC/CRREL TR-02-2, US Army Corps of Engineers, 40 pp.

Ho, D.V. and Meyer, R.E. 1962. Climb of a bore on a beach. Part 1: Uniform beach slope. *J. Fluid Mech.* <u>14</u>. 305-318.

Hughes, S.A. 2003. Wave momentum flux parameter for coastal structure design. Report No. ERDC/CHL CHETN-III-67, US Army Corps of Engineers, Vicksburg, MS., 12 pp.

International Code Council, INC. 2000. <u>International Building Code 2000.</u> Birmingham, AL. April.

International Code Council, INC. 2002. <u>International Building Code 2003.</u> Country Club Hills, IL.

International Conference of Building Officials. 1997. <u>1997 Uniform Building Code.</u> California. Appendix Chapter 31.

Matsutomi, H. & Shuto, N. 1994. Tsunami Engineering Technical Report No.11, DCRC, Tohoku University, 29-32.

Pacheco, K. H. & Robertson, I. N. 2005. Evaluation of Tsunami Loads and Their Effect on Reinforced Concrete Buildings. University of Hawaii Research Report.

Ramsden, J.D. 1993. Tsunamis: Forces on a vertical wall caused by long waves, bores, and surges on a dry bed. Report No. KH-R-54, W.M. Keck Laboratory, California Institute of Technology, Pasadena, Calif., 251 pp.

Shuto, N. 1994. Building damage evaluation for the 1993 Okushiri tsunamis, Tsunami Engineering Technical Report No.11, DCRC, Tohoku University, 11-28 (in Japanese).

Tonkin, S., Yeh, H., Kato, F., & Sato, S. 2003. Tsunami scour around a cylinder. <u>J. Fluid Mech.</u> <u>496</u>, 165-192.

UBC 1997. International Conference of Building Officials. <u>1997 Uniform Building Code</u>. California.

Wiegel, R.L. 1964. Oceanographical Engineering. Prentice-Hall, Inc. Englewood Cliffs, N.J., 532 pp.

Yeh, H. 2005. Maximum fluid forces in the tsunami runup zone. J. Waterway, Port, Coastal, and Ocean Engineering, ASCE, (under review).

Yeh, H.H., Ghazali, A., & Marton, I. 1989. Experimental study of bore runup. <u>J. Fluid Mech.</u> <u>206</u>, 563-578.

Appendix: Evaluation of a Prototype Reinforced Concrete building

Reinforced concrete buildings are typically designed based on consideration of dynamic forces associated with strong winds and earthquake effects. Tsunami effects are not normally considered. The objective of this appendix is to demonstrate how typical reinforced concrete buildings would perform under the conditions of tsunami loading. The following discussion is based on a research report by Pacheco & Robertson (2005). It must be noted that the sample evaluations are made using the existing tsunami-load guidelines; the improvements suggested in this report were not fully implemented in this study.

Pacheco & Robertson (2005) examined three prototype reinforced concrete buildings selected from Seismic and Wind Design of Concrete Buildings by Ghosh and Fanella (2003). Ghosh and Fanella provide detailed designs of five reinforced concrete buildings for wind and earthquake effects. The buildings are designed for specific seismic design categories (SDC). The SDC takes into account the seismic risk at the site of the structure, occupancy category of the structure, and soil characteristics at the site of the structure. The five reinforced concrete buildings incorporate various structural systems commonly used in the United States and are located in regions of low, moderate, and high seismic activity, and on different soil types. The buildings are designed according to the 2000 International Building Code (IBC 2000) which utilizes the SDC, the ASCE Standard "Minimum Design Loads for Buildings and Other Structures" (ASCE 7-98) and the 1999 edition of the Building Code Requirements for Structural Concrete (ACI 318-99). Typical locations and loading combinations considered in these prototype designs are given in Table A-1.

Table A-1. Prototype Building Locations

SDC	Wind Speed	Prototype Location	Equiv. Tsunami Prone Location
A	145	Miami, FL	Kauai, HI
B	90	Atlanta, GA	
C	110	New York, NY	Oahu & Maui, HI
D	85	San Francisco, CA	West Coast, US
E	85	Berkeley, CA	West Coast, US

While Pacheco & Robertson (2005) evaluated three of the five building types, we present only one of the three cases for demonstration purposes: the selected building is an office building with dual and moment-resisting frame systems. The material properties used in the prototype design are a 28-day compressive concrete strength of 4,000 psi, concrete density of 150 pcf and reinforcing steel yield strength of 60,000 psi.

The building is a twelve-story office building with dual shear wall-frame system in one direction, say the north-south direction, and a moment-resistant frame system in the other direction (east-west) as shown in Fig. A-1. Lateral forces are resisted by a combination of shear walls and frames acting simultaneously in the north-south direction. IBC 2000 allows a shear wall-frame interaction system with ordinary reinforced concrete moment frames and ordinary reinforced concrete shear walls for SDC A. For SDC C the dual system consist of intermediate moment frames and ordinary reinforced concrete shear walls. For SDC D and E the dual system must consist of special moment frames and special reinforced concrete shear walls. The distinction between ordinary, intermediate and special frames or walls relates to the reinforcement detailing required to ensure adequate ductility during the design seismic event.

In the east-west direction lateral forces are resisted by the flexural action of the beams and columns in the moment resisting frames. The use of an ordinary reinforced concrete moment frame is permitted for SDC A. Intermediate reinforced concrete moment frames can be used for SDC C but special reinforced concrete moment frames are required for SDC D and E.

Loading Conditions

The building is analyzed and designed for four of the prototype locations given in Table A-1. Depending on the location, the lateral framing system is analyzed for the appropriate wind and seismic loads. Sample beams, columns, and walls are then designed and detailed for the controlling load combination of gravity load, in combination with either wind or seismic forces.
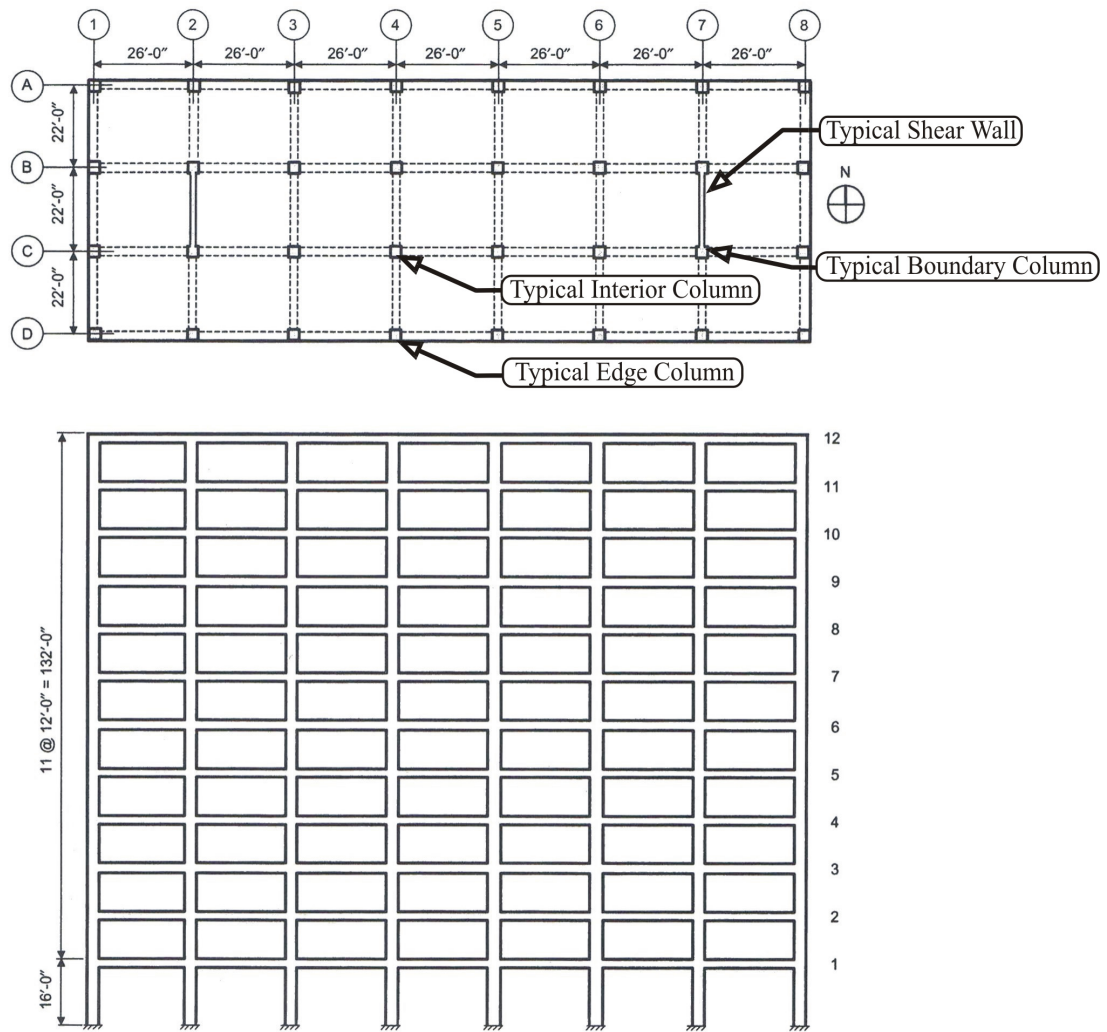
Figure A-1: Typical Plan and Elevation of Building 1

In Miami, Florida, the office building is assumed to be in site class D, with SDC A, and winds of 145 mph with exposure B. The structural components consist of 8-inch floor slabs, 24 x 24 inch beams, 28 x 28 inch columns and 12-inch thick shear walls. In New York City, the office building is designed for SDC C with a wind speed of 110 mph with exposure B. The member dimensions are 8-inch floor slabs, 22 x 22 inch beams, 26 x 26 inch interior columns, 24 x 24

inch exterior columns and 12-inch thick shear walls. In San Francisco, the office building is assumed to be SDC D with a wind speed of 85 mph with exposure B. The member dimensions are 8-inch floor slabs, 28 x 26 inch beams, 30 x 30 inch interior columns, 26 x 26 inch exterior columns, 36 x 36 inch boundary elements at each end of the 16-inch thick shear walls. In Berkeley, CA, the office building is assumed to be in SDC E with wind speed of 85 mph and exposure B. In this example additional shear walls are located along column lines 3 and 6 (Fig. A-1). The dimensions of the structural components are 8-inch floor slabs, 28 x 32 inch beams, 34 x 34 inch interior columns, 30 x 30 inch exterior columns, 40 x 40 inch boundary elements at each end of the 18-inch thick shear walls.

Evaluation for Tsunami Loading

Pacheco & Robertson (2005) analyzed the prototype structures subjected to three levels of tsunami flow, namely 3m, 5m and 10m above the ground floor level. Here we present only the case of 3m flow depth for demonstration purposes. Note that if the building is situated at an elevation of 2m above sea level, the 3m flow depth at the building site would be equivalent to a 5m tsunami, which is about the maximum observed in India for the recent 26 December 2004 Indian Ocean Tsunami. No attempt was made to evaluate the probability of these flow levels at any particular coastal location, or to use the flow conditions suggested in this report, i.e. (15) and (16). Rather, the intent was to evaluate the effects on a typical prototype building using the existing code guidelines. Based on this assumed flow depth, the code equations and loading combinations were used to compute flow velocity and the subsequent loads on the building or structural element under consideration. The building was evaluated for base shear of the entire structure and critical forces on individual structural elements at the lower levels induced by the tsunami flow. The structure was evaluated for tsunami inundation in the north-south direction and east-west direction separately. The general evaluation procedures are discussed below with application to the prototype building, designed for SCD A and 145mph winds (Miami, FL). For the higher SDC levels the calculations are similar to what is shown below (Pacheco & Robertson, 2005).

Calculating Base Shear for the Entire Structure

Tsunami loading combinations provided by FEMA 2000 and Dames & Moore (1980) were used for calculating base shear for the entire structure for the prototype buildings. Two cases were investigated to determine the base shear resulting from each tsunami flow depth.

Case 1: prototype buildings were modeled with breakaway walls at the lower levels that expose the structural components during the tsunami. Tsunami loads are applied to these structural members including columns, beams/floor slab and structural walls. The forces on each structural component were combined with a single impact force in order to determine the base shear for the entire structure. In Case 1 when the tsunami strikes the building in the north-south direction the shear walls are equivalent to columns since the walls are parallel to the flow of water (Fig. A-1). These forces are then combined with the loads on all other columns and beams impacted by the tsunami flow. For a tsunami in the east-west direction, the shear walls are now perpendicular to the flow. The resulting shear wall forces are combined with the loads on the columns and beams. The 3m tsunami impacts only the ground floor columns and shear walls. The tsunami in the N-S direction would impact 32 columns, while the E-W tsunami would impact 2 shear walls in addition to the 32 columns. The forces on each of the structural members are computed and

combined with a single impact load to determine the base shear for the entire structure for the tsunami being considered.

Case 2: the tsunami forces on the structure were computed as if the structure is built with non-breakaway walls at the lower levels. If all walls, windows, doors, etc. at the lower levels of the prototype building are assumed not to breakaway during the tsunami, then significantly larger tsunami loads would be anticipated. The building width for north-south tsunami flow is 184 feet 4 inches and 68 feet 4 inches for east-west tsunami flow. The two equations used for forces on this fully enclosed building are hydrodynamic and surge forces. The impact force is added at the top of the tsunami flow. Note that breaking-wave forces are not considered as we discussed in the report. The result which yields the greatest force on the structure is compared to the wind or seismic base shear used in the prototype building design.

Calculating Forces on Structural Members

Tsunami force loading combinations were applied to the ground floor columns and/or walls. Only the ground floor structural members were investigated because the tsunami forces are greatest at this level, and these members carry the greatest gravity loads. Failure of any of these members could lead to progressive collapse of a significant portion of the building.

The lateral tsunami loads were applied to the structural members using Enercalc Version 5.8, a structural analysis computer program (Enercalc 2004). The columns and walls were modeled with fixed end conditions at the foundation and the first floor. The dimensions of the individual member were input along with the tsunami forces for the particular structural member. The maximum bending moment, shear force and axial force were then compared with the seismic or wind induced design bending moment, shear force and axial force for the same member.

As is common in practice, many of the members in the prototype buildings have greater strength than actually required for the member forces induced by the seismic or wind loading. In order to evaluate the actual strength of the members, the as-built structural section properties and reinforcing steel layout were modeled in PCA Column, a computer program for design of reinforced concrete columns and walls (PCA 2004). This program determines the bending moment - axial load interaction diagram for the column or wall member. Given the maximum factored axial load on the column during the tsunami, the member bending moment capacity is determined from the interaction diagram. The moment capacity can then be compared with the bending moment applied by the tsunami loads. The as-built shear capacity of the column is calculated following the ACI Code procedure (ACI, 1999), and compared with the maximum factored shear force from the tsunami loads. The computation of member forces and as-built strengths is demonstrated for column C4 and the shear wall on Line 7 of the prototype building 1 (SDC A – Miami, FL) (Fig. A-2).

Type 1 Column Forces

The hydrodynamic force on a column is modeled as a uniform load from the column base to the top of the tsunami flow depth. The impact force is added at the top of the tsunami flow depth. Procedures for calculating these forces for Type 1 members with a 3m tsunami on prototype structure 1 (SDC A) are shown below. Similar computations were performed for the same column subjected to the other tsunami flow depths. The same procedure was then repeated for prototype structure 1 designed for other seismic design categories (Pacheco & Robertson, 2005).
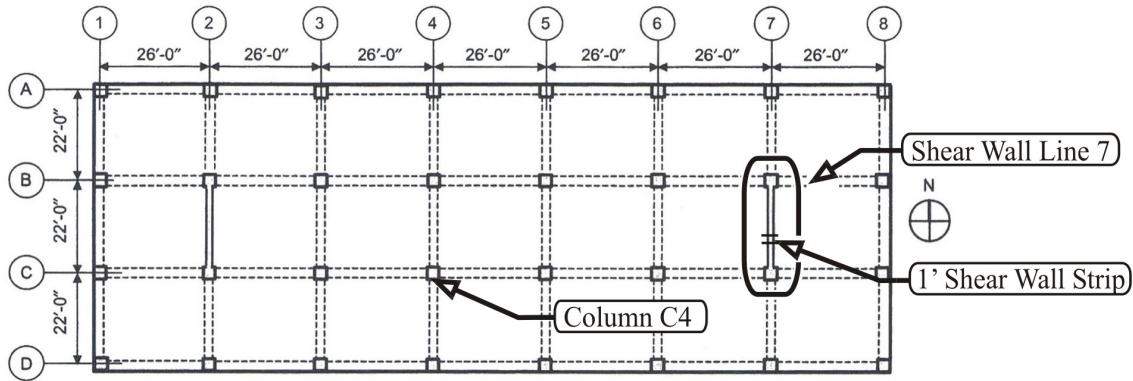
Figure A-2. Plan view of prototype building 1 showing members evaluated

An impact force is applied to the column in addition to the hydrodynamic force to simulate the effect of floating debris. The weight, velocity, duration and location of this debris impact are all defined by the codes. A sample calculation of the impact force for column C4 subjected to a 3 m tsunami flow is shown below.

$g = 32.17(\dfrac{ft}{\sec^2})$ Gravitational constant

$d_s = 9.842(ft)$ Tsunami flow depth (3 m)

$W = 1000(lb)$ Code assumed weight of debris

$V = 2\sqrt{g * d_s} = 35.59(\dfrac{ft}{\sec})$ Tsunami design flood velocity

$\Delta t = 0.1(\sec)$ Code assumed impact duration in seconds (Concrete member)

$F_i = \dfrac{WV}{g\Delta t} = \dfrac{1000 \times 35.59}{32.17 \times 0.1} = 11.06(kips)$ Impact force

The hydrodynamic force on the column is calculated as shown below.

$d_s = 9.842(ft)$ Tsunami flow depth (3 m)

$\rho = 1.99(\dfrac{lb * \sec^2}{ft^4})$ Mass density of water

$C_d = 2.0$ Drag coefficient for square column

$D = 2.333(ft)$ Column dimension

$A = D * d_s = 22.96(ft^2)$ Column exposed area

$g = 32.17(\dfrac{ft}{\sec^2})$ Gravitational constant

$$V = 2\sqrt{g * d_s} = 35.59(\frac{ft}{sec}) \quad \text{Tsunami design flood velocity}$$

$$F_d = \frac{1}{2}\rho C_d AV^2 = \frac{1}{2} \times 1.99 \times 2.0 \times 22.96 \times 35.59^2 = 57.88(kips)$$

This represents the total hydrodynamic force on the column. To determine the force per unit height of the column, the hydrodynamic force is divided by the tsunami flow depth as follows.

$$w_d = \frac{F_d}{d_s} = \frac{57.88}{9.842} = 5.88(\frac{kips}{ft})$$

The hydrodynamic force per unit height and the impact force acting at the top of the tsunami flow are then modeled as transverse loads applied to a fixed end column in Enercalc. The free height of the column is the distance from the ground floor to the bottom of the first floor beams (14 feet). Figure A-3 shows the Enercalc model of the column in a horizontal orientation. The base of the column (left end) is assumed fixed against lateral translation and rotation at the foundation. The top of the column (right end) is assumed fixed against lateral translation and rotation because of the continuity with the column above the first floor, and the restraint provided by the first floor beams and slab. The applied uniformly distributed hydrodynamic load and concentrated impact force are shown, along with the resulting maximum bending moments and shears in the column. Table A-2 shows the results of column C4 analysis for hydrodynamic wave loading in combination with the debris impact force for a 3m tsunami flow.

5.88 k/ft   11.06 k   5.88 k/ft

14 ft

Mmax = 49.83 k-ft @ 7.09 ft from bottom

Mmax @ bottom = -97.82 k-ft
Vmax @ bottom = 41.671 k

Mmax @ top = -85.82 k-ft
Vmax @ top = 27.260 k
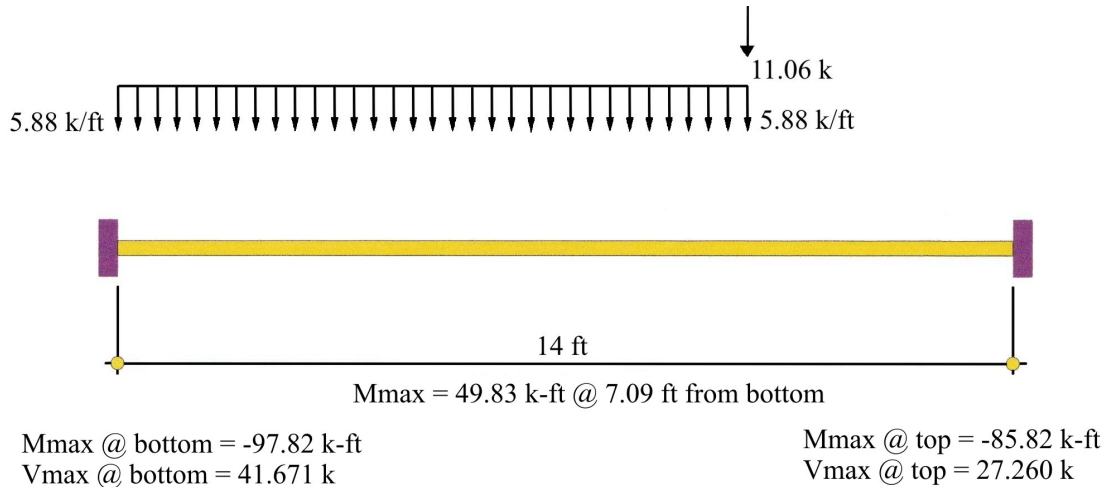
Figure A-3. Column analysis for hydrodynamic and impact forces

The axial force on this column is given by Ghosh and Fanella (2004) as 1,182.55 kips dead load and 146.18 kips live load reduced according to IBC 2000. The dead, live and tsunami loads are then factored by two different loading combinations. The maximum factored bending moment, shear force and axial force are then compared with the design forces due to wind and seismic loading.

Table A-2. Building 1 SDC A column results for tsunami force models

Building 1 - SDC A Column - Ground To First Floor		Bottom of Column	Middle of Column	Top of Column
Hydrodynamic Model	Bending Moment (ft-kips)	97.82	49.83	85.82
	Shear Force (kips)	41.67	0	27.26

In these loading combinations, the tsunami load is incorporated in the same way that wind loads are considered by Ghosh and Fanella.

The first loading combination is $0.75(1.4D + 1.7L + 1.7T)$ which incorporates the effects of dead load (D), live load (L) and tsunami load (T). The second loading combination is $0.9D + 1.3T$ which incorporates a reduced dead load and the tsunami force. The results are shown in Table A-3.

Table A-3. Summary of Loading Combinations for column C4.

Load Cases	Axial Force (kips)	Bending Moment (ft-kips)	Shear Force (kips)
Dead (D)	1,182.55	0.00	0.00
Live (L)	146.18	0.00	0.00
Tsunami (T)	0.00	97.82	41.67
Loading Combinations			
0.75(1.4D+1.7L+1.7T)	1,428.05	124.72	53.13
0.9D+1.3T	1,064.30	127.17	54.17

The maximum factored axial force, bending moment and shear force are then selected. In this example the maximum factored axial force is from the first loading combination. The maximum factored bending moment and shear force result from the second loading combination. Table A-4 lists the maximum factored loads for a 3m tsunami on column C4 for building 1 (SDC A).

Table A-4. Maximum 3 meter tsunami loading on column.

Column Ground to First Floor	Maximum Axial Force (kips)	Maximum Bending Moment (kips-foot)	Maximum Shear Force (kips)
3 Meter Tsunami	1428.05	127.17	54.17

These values are now compared with the design forces for which the members were designed based on seismic and wind loading. For building 1 SDC A, wind is the controlling factor in the design. Table A-5 shows the column forces from wind analysis along with the forces due to a 3m tsunami.

In Table A-5 the tsunami force cells are color-coded to indicate whether the column is adequate, marginal or inadequate. In this case, if the tsunami force is less than or equal to the design load, the member is adequate and the cell is shaded green. If the tsunami force exceeds the design force by up to 50%, the column is considered marginal since the load factors and strength reduction factors used in typical design result in an approximate safety factor against failure of 1.5. These cells are shaded yellow. If the member forces induced by the tsunami exceed 1.5 times the design forces, the member is considered inadequate and the cell is shaded red. This color-coding is used throughout this report for easier comparison of tsunami and design forces.

Table A-5. SDC A design forces and 3 meter tsunami forces

KEY		Column				
ADEQUATE		Max Axial	N-S Max	E-W Max	N-S Max	E-W Max
MARGINAL	SDC	Force	Bending Moment	Bending Moment	Shear Force	Shear Force
INADEQUATE		(kips)	(ft-kips)	(ft-kips)	(kips)	(kips)
*WIND (145 mph)	A	1,443.27	126.55	126.55	24.00	24.00
3 Meter Tsunami	A	1,428.05	127.17	127.17	54.17	54.17

Type 2 Wall Forces

Type 2 individual structural member loading conditions are obtained by calculating tsunami forces acting perpendicular to a wall. The conditions are hydrodynamic and surge forces perpendicular to the wall. The hydrodynamic force is modeled as a uniform load over the full height of the tsunami flow. The surge force is modeled as a triangular load with a maximum intensity at the base of the wall and decreasing to zero at the top of the tsunami flow depth. In combination with each of these hydraulic loads, the impact force introduced earlier is applied to the wall at the top of the tsunami flow depth. The wall capacity is determined in two ways. First, we consider the full geometric shape of the wall cross-section to resist the tsunami loads. Then, a 1-foot wide vertical strip of the wall is considered to resist the hydraulic loads only, without the impact force, to investigate the ability of the wall to span vertically between the foundation and first floor. This second analysis is particularly important for walls with a large aspect ratio of the horizontal wall dimension to the height of the wall between structural levels.

Hydrodynamic Force on Structural Wall

The hydrodynamic force applied by a 3 meter tsunami in the E-W direction to the structural shear wall (Fig. A-1) was computed in the same manner as the column except using $C_d = 1.25$, and $A = 239.49 \, ft^2$. The total hydrodynamic force on the wall is therefore:

$$F_d = \frac{1}{2}\rho C_d A V^2 = \frac{1}{2} \times 1.99 \times 1.25 \times 239.49 \times 35.59^2 = 377.27(kips)$$

The force on the wall from the hydrodynamic equation is equivalent to a uniformly distributed load over the depth of the tsunami flow of:

$$w_d = \frac{F_d}{d_s} = \frac{377.27}{9.842} = 38.33(\frac{kips}{ft})$$

The hydrodynamic force per unit length with the impact force acting at the top of the tsunami flow was then modeled in Enercalc as shown in Fig. A-4. The wall is modeled with fixed ends at the foundation and first floor level, resulting in the maximum bending moments and shear forces.

11.06 k

38.33 k/ft   38.33 k/ft

14 ft

Mmax = 288.28 k-ft @ 6.76 from bottom

Mmax @ bottom = -584.71 k-ft
Vmax @ bottom = 258.706 k

Mmax @ top = -434.07 k-ft
Vmax @ top = 129.627 k
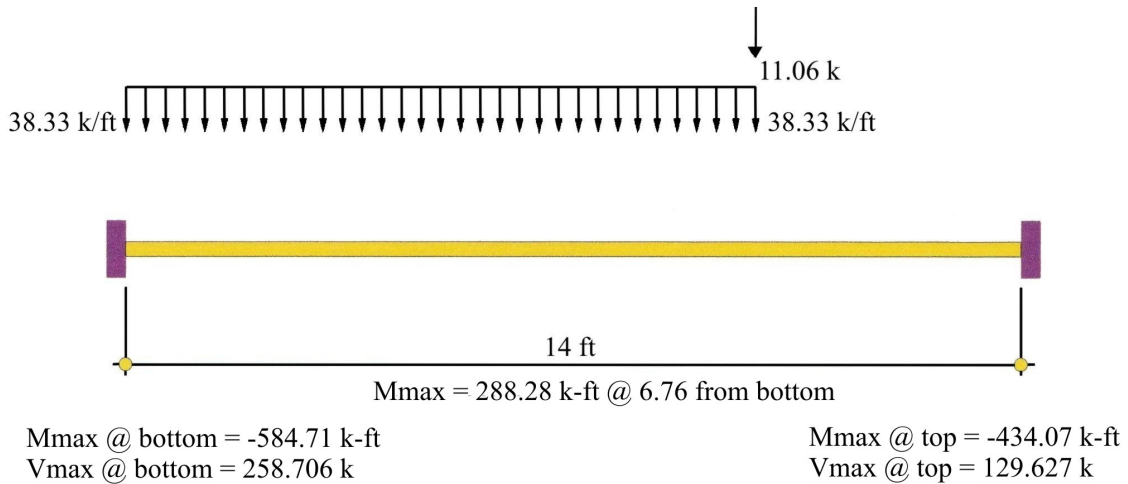
Figure A-4. Prototype building (SDC A) with hydrodynamic and impact force on wall

Surge Force on Structural Wall

The surge force acting on the wall is calculated using the tsunami flow depth. Based on Dames & Moore (1980) the surge force on a wall is modeled as a triangular force, with the total load given by:

$$F_s = f_s * w$$

where: $w = 24.333(ft)$ width of wall

$$f_s = 4.5\gamma d_s^2$$

$$\gamma = 64.0(\frac{lb}{ft^3})$$ weight density of sea water

$$d_s = 9.842(ft)$$ tsunami flow depth

$$\therefore f_s = 4.5\gamma d_s^2 = 4.5\times 64\times 9.842^2 = 27.9(\frac{kips}{ft})$$

and, $F_s = f_s * w = 27.9 * 24.333 = 678.8(kips)$

As discussed in this report, this estimate likely yields excessively conservative value.

The force per unit height at the base of the tsunami is calculated as follows:

$$F_s = 9\gamma d_s w = 9\times 64\times 9.842\times 24.333 = 137.94(\frac{kips}{ft})$$

Figure A-5 shows the surge and impact loading on the structural wall, along with the maximum bending moments and shears induced in the wall.

137.94 k/ft

11.06 k

14 ft

Mmax = 385.94 k-ft @ 5.72 ft from bottom

Mmax @ bottom = -1,001.19 k-ft
Vmax @ bottom = 560.593 k

Mmax @ top = -475.32 k-ft
Vmax @ top = 129.284 k

Figure A-5. E-W 3 meter surge force and impact force on wall

The bending moments and shear forces which result from either the hydrodynamic or surge force models are listed in Table A-6. The surge model yields the larger values of bending moment and shear force of 1,001.19 ft kips and 560.59 kips, respectively. The axial force due to dead and live loads are 2,716 kips and 279 kips, respectively, as determined by Ghosh and Fanella (2004). These forces are combined using two factored load combinations. The first loading combination is $0.75(1.4D + 1.7L + 1.7T)$. The second loading combination is $0.9D + 1.3T$ which incorporates the axial dead load and the tsunami force. The results are summarized in Table A-7.

Table A-6. Wall results for tsunami force models

Building 1 - SDC A Wall - Ground To First Floor		Bottom of Wall	Middle of Wall	Top of Wall
Hydrodynamic Model	Bending Moment (ft-kips)	584.71	288.28	434.07
	Shear Force (kips)	258.71	0.00	129.63
Surge Model	Bending Moment (ft-kips)	1,001.19	385.94	475.32
	Shear Force (kips)	560.59	0.00	129.28

Table A-7. Summary of Loading Combinations for (1-A) Wall

Load Cases	Axial Force (kips)	Bending Moment (ft-kips)	Shear Force (kips)
Dead (D)	2,716.00	0.00	0.00
Live (L)	279.00	0.00	0.00
Tsunami (T)	0.00	1,001.19	560.59
Loading Combinations			
0.75(1.4D+1.7L+1.7T)	3,207.53	1,276.53	714.75
0.9D+1.3T	2,444.40	1,301.55	728.77

The maximum factored axial force results from the first loading combination while the maximum factored bending moment and maximum factored shear force result from the second loading condition. These values are listed in Table A-8

Table A-8. Maximum 3 meter tsunami loading on (1-A) Wall

Wall Ground To First Floor	Maximum Axial Force (kips)	Maximum Bending Moment (kips-foot)	Maximum Shear Force (kips)
3 Meter Tsunami	3,207.53	1,301.55	728.77

The resulting wall capacities are compared with the factored loads due to a 3-meter tsunami flow depth in Table A-9. In this case, all tsunami loads are less than the wall capacity, except for shear which is marginal.

Table A-9. 3 Meter tsunami forces with As-Built Wall Capacity

KEY		As-Built Shear Wall - Ground To First Floor		
ADEQUATE		Max Axial	E-W Max Bending	Max Shear
MARGINAL	SDC	Force	Moment Capacity	Strength
INADEQUATE		(kips)	(ft-kips)	(kips)
*WIND (145 mph)	A	3,208.00	2,856.00	562.43
3 Meter Tsunami	A	3,207.53	1,301.55	728.77

Comments:

As we mentioned, Pacheco & Robertson (2005) computed the performance of three typical prototype building structures under three tsunami conditions, i.e. 3m, 5m, and 10m tsunami flow depths at the building site. They concluded that, 1) the prototype building with moment-resisting frame or dual system was able to resist the tsunami forces; 2) the prototype building with shear wall-frame system was able to resist the tsunami forces, however individual shear walls perpendicular to the tsunami flow may fail and lead to progressive collapse of the building; and 3) bearing wall buildings, which utilize relatively thin walls to support all gravity and lateral loads, are likely to perform poorly during a tsunami event.

Because there are still many uncertainties with respect to tsunami forces, which need further improvements of the evaluation procedure, we cautiously state here that the evaluation based on the present code indicates that a typical reinforced-concrete building can survive a 3-m tsunami flow depth. Note that the 3-m flow depth at the building located at 2 m above the sea level can be interpreted as a 5-m tsunami runup. This is consistent with the empirical data shown in Fig. 7.